A Compact Multi-Band MIMO Antenna with High Isolation for C and X Bands Using Defected Ground Structure

Negin POUYANFAR [1], Changiz GHOBADI [1], Javad NOURINIA [1], Kioumars PEDRAM [1], Maryam MAJIDZADEH[2]

[1] Electrical Engineering Dept., Urmia University, Urmia, Iran
[2]Dept. of Electrical and Computer Engineering, Urmia Girls Faculty, West Azarbaijan branch, Technical and Vocational University (TVU), Urmia, Iran

n.pouyanfar@urmia.ac.ir, ch.ghobadi@urmia.ac.ir, j.nourinia@urmia.ac.ir, pedram.qmars@gmail.com, mmajidzadeh@tvu.ac.ir

Submitted January 4, 2018 / Accepted May 8, 2018

Abstract. *A compact multi-band multi-input multi-output (MIMO) antenna with high isolation is proposed for C and X bands applications. The antenna consists of two trapezoidal-shaped patches printed on FR-4 substrate with a thickness of 1.6 mm and compact size of 17 × 42 mm^2. Defected ground structure (DGS) is wisely embedded in antenna body to reduce the mutual coupling between the antenna elements. This modification suitably enhances the isolation by 30 dB in C-band extended from 6.6 GHz to 7.6 GHz and by 17 dB in X-band between 8.3 GHz to 10 GHz. Moreover, five meander line rectangular patches are properly included to further improve the mutual coupling and eliminate the antenna size increment, simultaneously. The aforementioned meander lines also improve impedance bandwidth of the antenna as well as impedance matching over the entire frequency band. Close agreement of simulated and measured results confirms the antenna outperformance. Design, simulation, and performance analysis of the proposed antenna is discussed in detail.*

Keywords

Multi-Input Multi-Output (MIMO), Defected Ground Structure (DGS), mutual coupling, C band, X band

1. Introduction

The soaring demands for high quality data transmission have brought up the multi-input multi-output (MIMO) antenna technology as an attractive choice for antenna designers. Recently MIMO technology has been widely deployed to increase channel capacity and signal quality in array antennas. In this configuration, mutual coupling between adjacent elements considerably affects antenna system performances [1]. Accordingly, one of the critical challenges in MIMO systems is to obtain high isolation and low correlation between different elements to increase the channel capacity and subsequently attain good spectral efficiency and higher gain. The conventional approach for reducing mutual coupling is to place antennas in a properly far-away distance, usually half the wavelength, far from each other. By this approach, the elements have the minimum effect on each other. Although this approach ends in good results, it requires a large space which would not be suitable for handheld wireless devices. With the aim of higher reliability and functionality, several techniques have been recently introduced to minimize the inter-element coupling and therefore increase isolation. For instance, a completely planar electromagnetic band gap (EBG) structure has been proposed for mutual coupling reduction in [2–4]. High Impedance Surfaces (HISs) and Artificial Magnetic Surfaces (AMCs) are employed with the goal of miniaturization and antenna performance improvement [5]. However, due to the emerged electrical loss as a result of using vias and also a large occupied area, these structures are not suitable solutions. Moreover, in [6], [7], slots with different lengths etched on the radiating patch or the ground plane have led to high isolation. Besides, some other approaches are tried in this context which are briefly reviewed as follows: A wideband neutralization line has been applied in [8]; the symmetric arrangement of the antenna elements and its effect on mutual coupling reduction was tailored in [9]; implementation of slotted meander line resonator achieved by creating slot in the ground plane was scrutinized in [10]; modified serpentine structure (MSS) was deployed as a band reject filter in [11]; eventually, the defected ground structures (DGSs) [12], [13] have been proposed to model inductance and capacitance behavior, limit the surface waves between the antenna elements and consequently decrease the mutual coupling. Accordingly, the isolation feature is increased in MIMO systems. Although DGSs yield mutual coupling reduction, they increase the structural complexity. Similar configuration to meander lines in [14] and other useful techniques have

been surveyed to attain better results in MIMO systems as reported in [15]. In this way, a broadband decoupling has been achieved through two types of transmission lines based on the substrate integrated waveguide (SIW) and miniaturized Spoof Surface Plasmon Polariton (SSPP). Electromagnetic and specifically mantle cloaking can also be tapped for further mitigation of mutual coupling associated with densely packed antennas in overcrowded mobile communication systems. Deployment of metasurfaces in this technique yields lightweight and very thin structures at microwave and radio frequencies [16–18]. The mutual coupling reduction which is achieved through properly engineered metal covers, makes the desired element invisible to others; therefore, it increases the system performance.

Dealing with mutual coupling reduction and increasing the isolation feature, this manuscript proposes a new design of an antenna for multi-band MIMO applications with increased functionality. The proposed antenna comprises of two trapezoidal-shaped patches printed on FR-4 substrate. Subsequently, DGS is wisely embedded in antenna body to reduce the mutual coupling between the antenna elements. This modification suitably enhances the isolation in C and X-band. In other words, the isolation between the antenna elements is augmented by employing DGS. Moreover, five meander line rectangular patches are properly included to further improve the mutual coupling and eliminate the antenna size increment, concurrently. The aforementioned meander lines also improve impedance bandwidth of the antenna as well as impedance matching over the entire frequency band. Moreover, the proposed configuration fulfills the typical properties of a MIMO system such as the envelope correlation coefficient (ECC) and diversity gain. To provide a detailed study, design procedure along with theoretical concepts, simulations, and experimental results are presented and compared with each other. The obtained results are interrogated in terms of size and bandwidth which corroborate outperformance of the proposed design. Further analysis is provided through the manuscript body.

This paper is organized as follows: Section 2 presents antenna design steps and analysis of the DGS and its effect on antenna performance. Besides the parametric studies, surface current distribution, ECC, and some other important parameters are also presented and discussed. Experimental results are provided in Sec. 3 and compared with those of the simulation results. To shed light on the advantages of the proposed design, a comparative study with some of the previously designed antennas is reported in Sec. 4. As the ending point, a conclusion is drawn in Sec. 5.

2. Antenna Design and Performance Analysis

This section provides step by step design procedure of the proposed MIMO antenna. The 2-dimensional (2-D) configuration of the proposed antenna is shown in four steps in Fig. 1. As can be seen, the proposed antenna is fed by a single 50Ω microstrip line designed on FR-4 substrate with $\varepsilon_r = 4.4$, loss tangent of 0.025, and thickness of 1.6 mm. As shown in Fig. 1, the basic design structure, namely Ant. a, is composed of a simple trapezoidal-shaped patch and a ground plane on the backside. Subsequently, another trapezoidal-shaped patch is wisely embedded face to face with the first one (Ant. b). The aforementioned two patches are connected to each other through five rectangular conductors. In the next step, named as Ant. c, the above-mentioned five rectangular conductors are meandered with the aim of impedance bandwidth enhancement. Finally, in Ant. d, by introducing defects in the ground plane, the design of the proposed structure is finalized. To explore the final design in detail, the geometry and exact parameter values of the proposed antenna are illustrated in Fig. 2(a). As mentioned earlier, two connected trapezoidal-

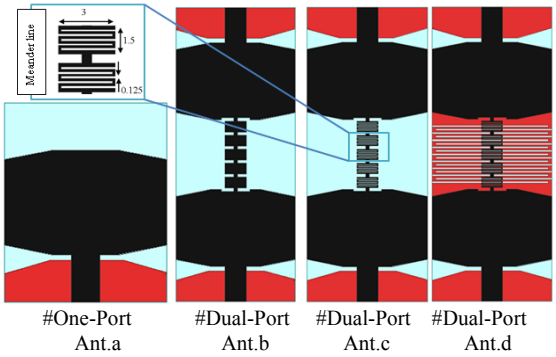

Fig. 1. Design procedure of the proposed multi-band MIMO antenna.

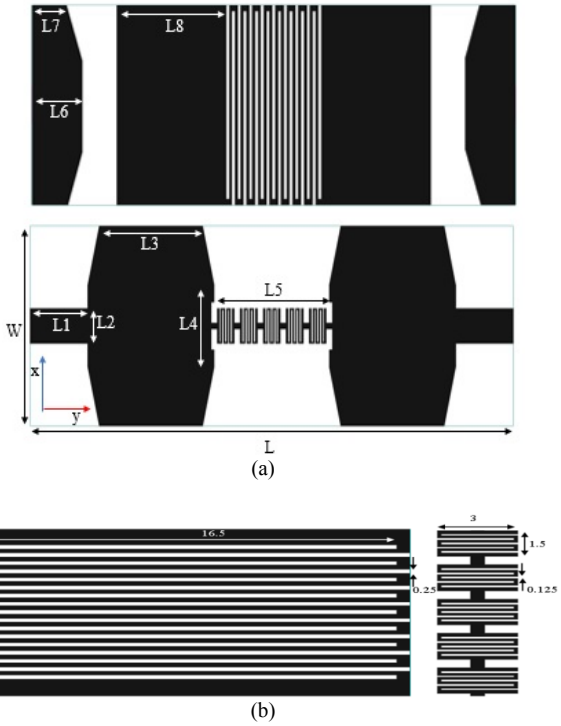

Fig. 2. Proposed antenna configuration: (a) Top and bottom view, (b) detailed geometry of the meander lines.

Parameter	Value	Parameter	Value
W	17	L4	7
L	42	L5	10
L_1	5	L6	4.375
L_2	3	L7	3
L_3	9	L8	9.25

Tab. 1. Dimensions of the proposed structure (All values are in mm).

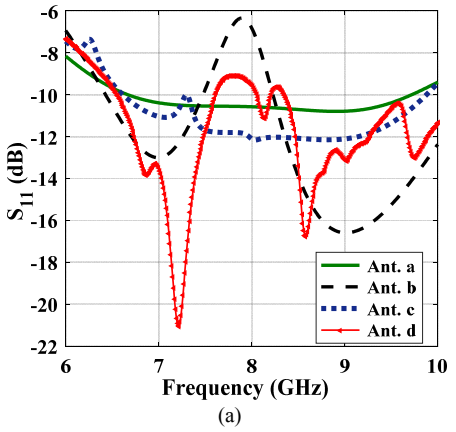

(a)

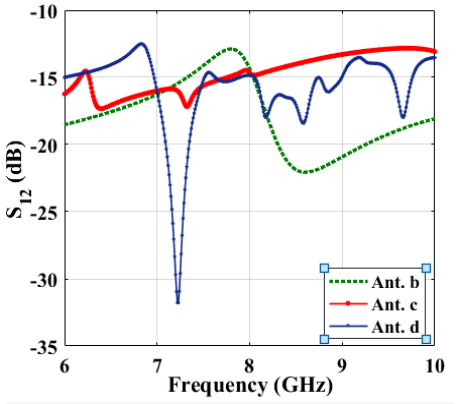

(b)

Fig. 3. Simulated S-parameters of the proposed antenna: (a) S_{11}, (b) S_{12} curve.

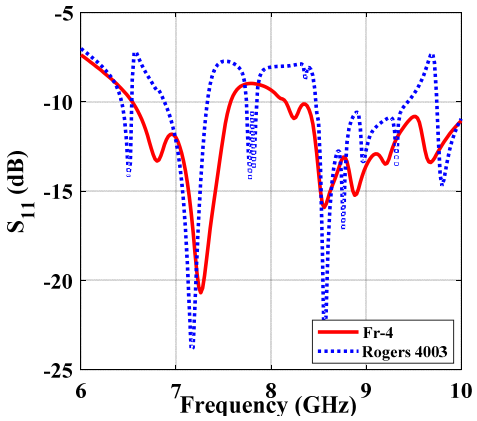

Fig. 4. Simulated S_{11} curves of the proposed antenna with FR-4 and Rogers-4003 substrate materials.

shaped patch with five rectangular meandered conductors are adapted to realize the desired functionality. Moreover, detailed information regarding the meandered lines is surveyed in Fig. 2(b). The optimal realized dimensions of the proposed structure are reported in Tab. 1.

Ansoft High Frequency Structure Simulator (HFSS) is employed to analyze the aforementioned structures in Fig. 1. Simulation results including S_{11} and S_{12} curves have been depicted in Fig. 3. Analyzing the S_{11} curves in Fig. 3(a) indicates that Ant. a, which is composed of a single antenna, covers the frequency band of 6.8 GHz to 9.6 GHz. In Ant. b, by including the other patch and connecting the conductive elements, the structure has lost its bandwidth between 7.5 GHz and 8.2 GHz compared to the single patch case (Ant. a) according to the results shown in Fig. 3(b). Meandering the conductive elements between the antenna elements in Ant. c yields impedance matching improvement; however, the mutual coupling needs to be further enhanced in the upper bands. Eventually, by introducing defects in the ground plane in the shape of meander lines (Ant. d), both impedance bandwidth and isolation are enhanced, simultaneously. S_{12} curves are also plotted in Fig. 3 (b). Due to the symmetrical structure of the proposed antenna, the simulated results of S_{22} and S_{21} are not depicted for brevity.

As it was mentioned earlier, FR-4 material is selected as the substrate in the proposed design. This selection is mainly due to its easy accessibility, low cost, and suitable performance. To investigate the effect of different substrate materials on the antenna performance, a comparison is made in Fig. 4 for FR-4 and Rogers-4003 regarding the S_{11} curves. It is clearly seen that the desired performance is obtained for FR-4 substrate; hence, by launching a trade-off among cost, accessibility and dielectric loss, FR-4 substrate exhibits superior characteristics. The agreement of the simulated and measured results confirms the successful performance of this material in the present design.

2.1 On the Effect of Defected Ground Structure (DGS)

The DGSs are equivalent to the LC circuits. By etching defects in the ground planes, in fact a band-stop filter is made for surface waves which consequently results in

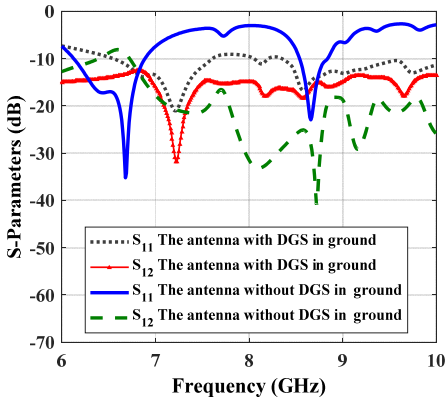

Fig. 5. Simulated S_{11} and S_{12} parameters of the proposed antenna with and without DGS in ground plane.

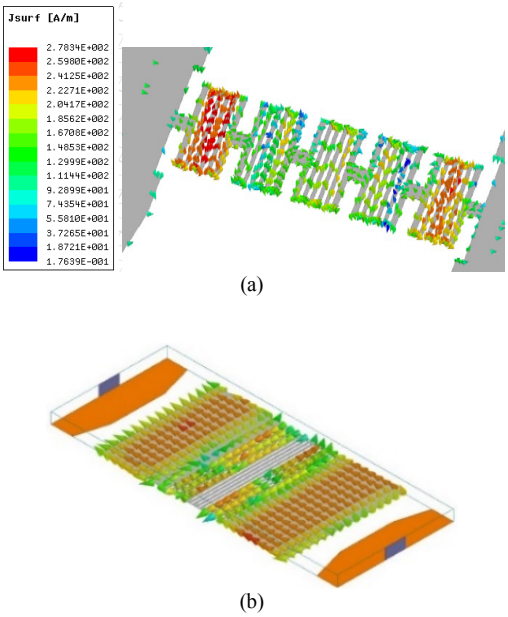

(a)

(b)

Fig. 6. Surface current distributions at 7.25 GHz in the meander line radiating patch, (b) in the meander line ground.

inter-element coupling reduction and isolation increment in MIMO systems. To verify this issue, the DGS filter is designed with the aim of making a stop-band in 7.2 GHz which is the desired operating frequency of the proposed antenna. The proposed DGS is designed by making a rectangular patch meandered. The effect of including DGS in the ground is clearly shown in Fig. 5. Higher isolation achievement is obviously confirmed. Clearly, by including the DGS, a better than –30dB isolation is achieved.

2.2 Surface Current Distribution

To verify the filtering characteristic of the DGS, surface current distribution of the designed antenna in 7.25 GHz is investigated in this section. As can be seen in Fig. 6, current vectors are mostly concentrated on the first and last meander line patches, gradually weakening toward the center part. The same phenomenon is observed for the ground plane; the concentration of the surface currents is strong on the right and left sides of the meandered line and it attenuates while moving toward the center of the defected ground plane. This notice suitably justifies the isolation provided between two elements at the favorable frequency.

2.3 Envelope Correlation Coefficient (ECC)

Envelope Correlation Coefficient (ECC) and diversity gain investigation would be useful to confirm the MIMO system applicability. ECC and diversity gain are related to each other such that by increasing the isolation or accordingly decreasing the coupling between elements, the diversity gain increases, and vice versa. The correlation coefficient between antenna elements is shown by ρ_e and is calculated in terms of scattering parameters as reported in (1) [19].

$$\rho_e = \frac{\left|S_{11}^* S_{12} + S_{21}^* S_{11}\right|^2}{\left(1-\left(\left|S_{11}\right|^2+\left|S_{21}\right|^2\right)\right)\left(1-\left(\left|S_{22}\right|^2+\left|S_{12}\right|^2\right)\right)} \quad (1)$$

where S_{11} is the reflection coefficient from port 1 when port 2 is connected to a matched load (i.e. there is no incident wave impinging the opposite port). Additionally, S_{21} is transmission coefficient from port 1 to port 2 under the same matching condition. Similar definitions are applied to S_{22} and S_{12}, with the only difference on port excitation order.

Figure 7(a) shows the envelope correlation for the proposed antenna. In practical applications, less than 0.5 ECC is considered as a suitable performance. It is clearly seen that the designed structure fulfills the requirements for MIMO systems by providing less than 0.015 for this parameter over the operating frequency band. Moreover, the ECC for the design steps of b, c, and d in Fig. 1, is depicted in Fig. 7(b). It is obvious that through a suitable modifying of design configuration, better ECC is obtained in each step.

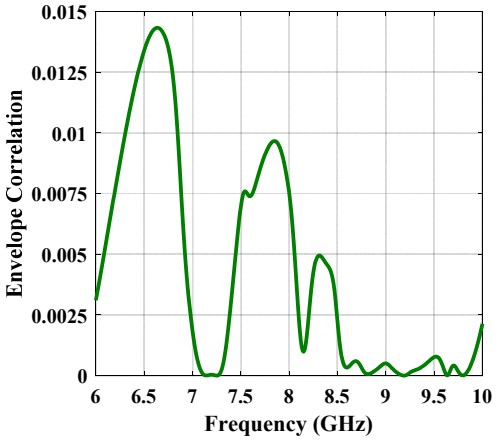

(a)

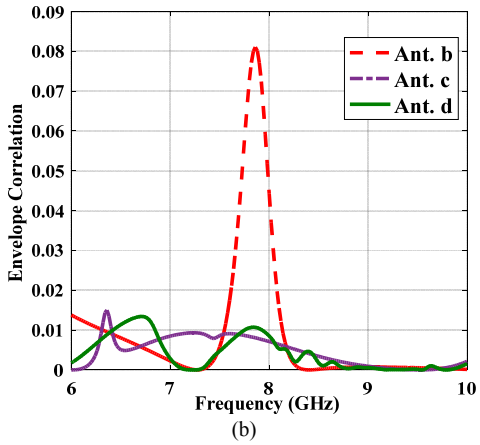

(b)

Fig. 7. (a) Calculated ECC for the proposed antenna, (b) ECC for different design steps shown in Fig. 1.

2.4 Diversity Gain

The next parameter to study is diversity gain. This parameter is shown by G_{app} and is defined as below [19]:

$$G_{app} = \sqrt{1 - |\rho_e|}. \quad (2)$$

Calculated diversity gain curve is shown in Fig. 8(a) which indicated values more than 9.9 through the entire frequency band. The obtained values satisfy the requirements of MIMO systems applications. Step by step improved diversity gain is obtained as illustrated in Fig. 8(b) for the antennas introduced in design steps introduced in Fig. 1.

2.5 Gain and Efficiency

The simulated gain of the designed structure is plotted in Fig. 9(a). It indicates that in the lower and higher resonances, namely 7.2 GHz and 8.5 GHz, more than 5 dB and about 1.7 dB gain are obtained, respectively. This achievement fulfills the requirements of MIMO communication systems applications. Moreover, the simulated efficiency of the proposed structure is provided in Fig. 9(b). More than 80% and 70% efficiency is observed in the lower and higher resonances, respectively.

2.6 Radiation Pattern

The radiation patterns of the proposed antenna in E-plane and H-plane at 7.2 GHz and 8.57 GHz are shown in Fig. 10, when one port is excited and the other is matched to a 50 Ω load. As can be seen, the radiation pattern E_φ is omnidirectional in both specified frequencies, while E_θ is bidirectional. Due to the symmetric structure of the proposed antenna, a stable radiation pattern is achieved which is suitable for use in communication systems.

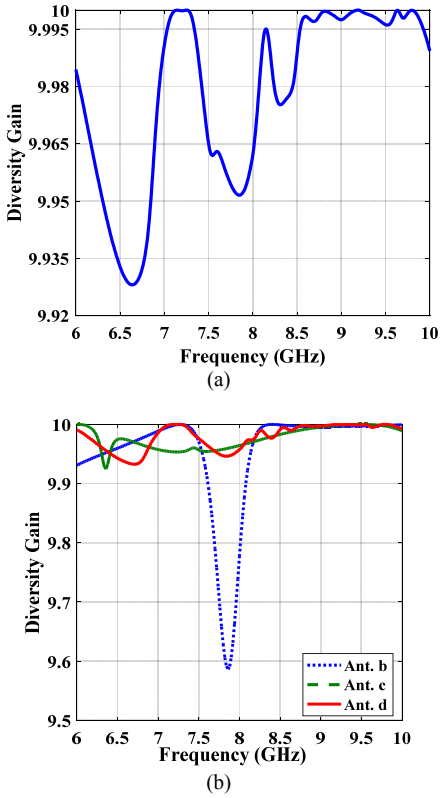

Fig. 8. (a) Calculated diversity gain for the proposed antenna. (b) Diversity gain for antennas b, c and d.

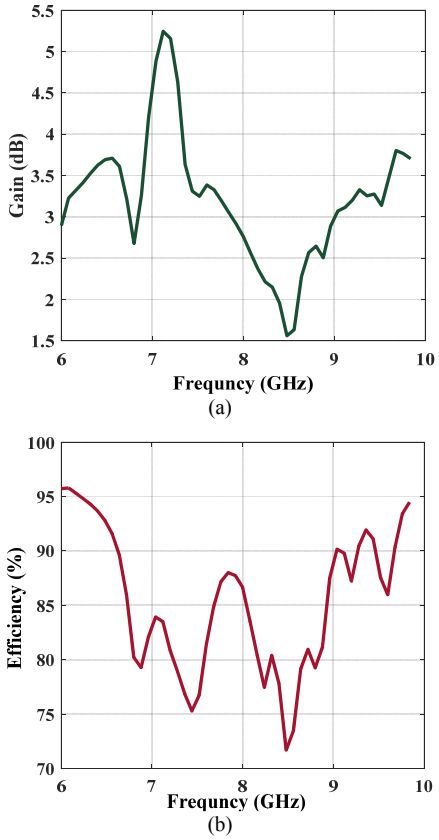

Fig. 9. (a) Simulated gain, (b) simulated efficiency of the proposed structure.

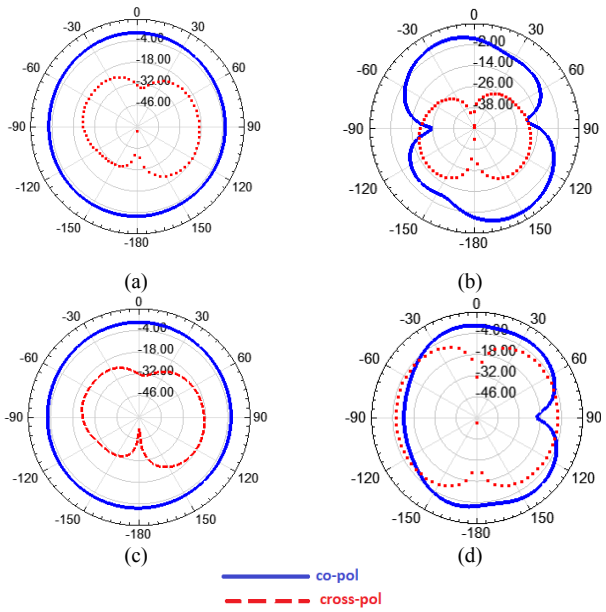

Fig. 10. The radiation patterns when one port is excited: (a) E-plane in 7.2 GHz, (b) H-plane in 7.2 GHz, (c) E-plane in 8.57 GHz, (d) H-plane in 8.57 GHz.

2.7 Parametric Study

This section establishes a parametric study to discuss the effect of different parameters variations on the antenna performance.

2.7.1 Analyzing the Effect of Ground Plane Length

The first important parameter with effective influence on the antenna performance is the length of the ground plane, denoted by L_7 in Fig. 2(a). Simulated S_{11} and S_{12} curves based on three different values of L_7 are plotted in Fig. 11. The results indicate that by increasing L_7 from 2 mm to 4 mm, the impedance bandwidth deteriorates, while the isolation is improved. Focusing on the mutual coupling reduction between antenna elements, $L_7 = 3$ mm is selected to satisfy both impedance bandwidth and a good isolation.

2.7.2 Analyzing the Effect of Center Rectangular Patch

The length of the center rectangular patch on the ground plane, namely L_8 in Fig. 2(a), is the other parameter to be studied. The simulated S_{12} curve for three values of L_8 presented in Fig. 12, shows that by increasing L_8 from 8.75 mm to 9.25 mm, better isolation is provided in a wider bandwidth. Further increasing this parameter to 9.75 mm deteriorates the isolation, more specifically in lower bands. To satisfy high isolation and accordingly less mutual coupling, $L_8 = 9.25$ mm is selected as an optimal value.

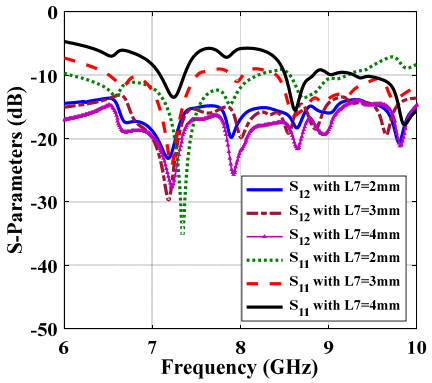

Fig. 11. Simulated S_{11} and S_{12} curves for different L_7 values.

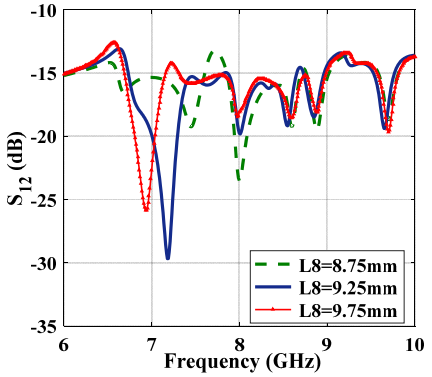

Fig. 12. Simulated S_{12} for the proposed antenna with different L_8 values.

3. Experimental Results and Discussion

To investigate the applicability of the proposed antenna, a prototype is fabricated, as illustrated in Figs. 13 (a) and (b). S_{11} and S_{12} parameters are measured by Agilent vector network analyzer PNA E8363C. The test is carried out when one port is excited and the other one is matched to the 50Ω load. The comparison between simulation and test outcomes is presented in Fig. 13 (c). Results indicate good agreements. The slight discrepancies are mainly caused by fabrication tolerances and probably due to differences in relative permittivity of the practical substrate compared to the simulated one which cannot be avoided.

4. Performance Comparison

To assess the performance of the proposed design, a comparison is carried out based on the data summarized in Tab. 2. Investigating the provided data in this table reveals a wider bandwidth and higher inter-element isolation for the proposed design which yields a compact and effective

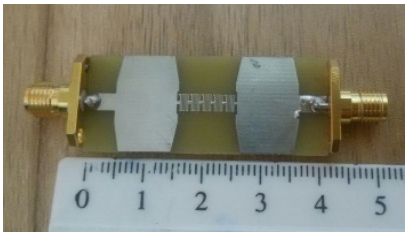

(a)

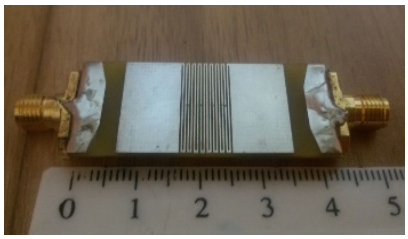

(b)

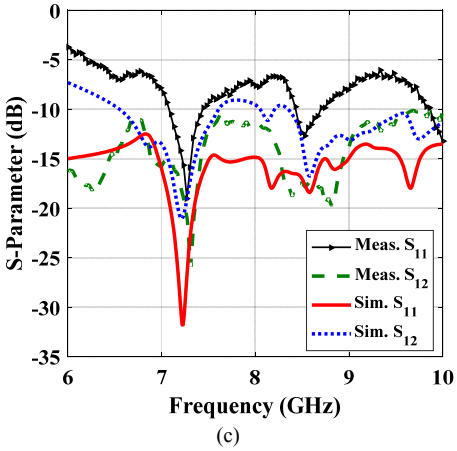

(c)

Fig. 13. The prototype fabricated antenna: (a) top view, (b) bottom view, (c) measured and simulated S-parameters.

Ref.	Size(mm^2)	B.W. %	S_{12} (dB)	f_0 (GHz)
[7]	60 × 95	≈25.25	≥ 15	1.75, 2.5
[8]	40 × 40	58.6	≥ 11	2.7
[9]	54 × 45	31.5	≥ 16	4.8
[10]	40 × 72	19.6, 16.1, 12.01	≥ 10	2.4, 4.6
Proposed Antenna	17 × 42	25.45	≥ 13	7.2, 8.57

Tab. 2. Performance comparison of the proposed antenna with the existing solutions.

structure. Moreover, the size of the proposed antenna is considerably reduced compared to the other antennas reported in [7–10]. This feature is mainly attributed to DGS utilization. It is also worth noting that the antennas in [8] and [10] provide only a single resonance although having larger size.

5. Conclusion

A compact MIMO antenna with good inter-element isolation was proposed, discussed, and measured. The antenna has a compact size of 17×42 mm^2 printed on a FR-4 substrate with 1.6 mm thickness. Two trapezoidal-shaped patches were connected through five meander line rectangular patches. Moreover, DGS was utilized to realize low coupling between antenna elements. The simulated and measured scattering parameters and surface current distribution analysis revealed that the DGS acts like a stop band filter. Approximate omnidirectional radiation patterns along with small ECC confirmed the high isolation in the proposed MIMO system. The satisfactory obtained characteristics make the proposed structure suitable for X- and C-bands application.

References

[1] FLETCHER, P., DEAN, M., NIX, A. Mutual coupling in multi-element array antennas and its influence on MIMO channel capacity. *Electronics Letters*, 2003, vol. 39, no. 4, p. 342–344. DOI: 10.1049/el:20030219

[2] ABDALLA, M. A., ABDELRAHEEM, A. M., ABDEGELLEL, M. H., et al. Surface wave and mutual coupling reduction between two element array MIMO antenna. In *IEEE Antennas and Propagation Society International Symposium (APSURSI)*. Orlando (FL, USA), 2013, p. 178–179. DOI: 10.1109/APS.2013.6710750

[3] RAJO-IGLESIAS, E., QUEVEDO-TERUEL, O., INCLAN-SANCHEZ, L. Mutual coupling reduction in patch antenna arrays by using a planar EBG structure and a multilayer dielectric substrate. *IEEE Transactions on Antennas and Propagation*, 2008, vol. 56, no. 6, p. 1648–1655. DOI: 10.1109/TAP.2008.923306

[4] NAIDU, P. R. T., KRISHNA, K. V., SHAIK, L. A., et al. Enhancement of isolation in printed MIMO antenna using multiple EBG elements. In *IEEE Applied Electromagnetics Conference (AEMC)*. Guwahati (India), 2015, p. 1–2. DOI: 10.1109/AEMC.2015.7509212

[5] PALANDOKEN, M. Artificial materials based microstrip antenna design. Chapter in Nasimuddin, N. (ed.) *Microstrip Antennas*. InTechOpen, 2011. DOI: 10.5772/14908

[6] TAO, J., FENG, Q. Compact ultrawideband MIMO antenna with half-slot structure. *IEEE Antennas and Wireless Propagation Letters*, 2017, vol. 16, p. 792–795. DOI: 10.1109/LAWP.2016.2604344

[7] DENG, J-Y., GUO, L-X., LIU, X-L. An ultrawideband MIMO antenna with a high isolation. *IEEE Antennas and Wireless Propagation Letters*, 2016, vol. 15, p. 182–185. DOI: 10.1109/LAWP.2015.2437713

[8] WANG, Y., DU, Z. A wideband printed dual-antenna system with a novel neutralization line for mobile terminals. *IEEE Antennas and Wireless Propagation Letters*, 2013, vol. 12, p. 1428–1431. DOI: 10.1109/LAWP.2013.2287199

[9] SARKAR, D., SRIVASTAVA, K. V. A compact four-element MIMO/diversity antenna with enhanced bandwidth. *IEEE Antennas and Wireless Propagation Letters*, 2017, vol. 16, p. 2469–2472. DOI: 10.1109/LAWP.2017.2724439

[10] ALSATH, M. G. N., KANAGASABAI, M., BALASUBRAMANIAN, B. Implementation of slotted meander-line resonators for isolation enhancement in microstrip patch antenna arrays. *IEEE Antennas and Wireless Propagation Letters*, 2013, vol. 12, p. 15 to 18. DOI: 10.1109/LAWP.2012.2237156

[11] ARUN, H., SARMA, A. K., KANAGASABAI, M., et al. Deployment of modified serpentine structure for mutual coupling reduction in MIMO antennas. *IEEE Antennas and Wireless Propagation Letters,* 2014, vol. 13, p. 277–280. DOI: 10.1109/LAWP.2014.2304541

[12] HABASHI, A., NOURINIA, J., GHOBADI, C. A rectangular defected ground structure (DGS) for reduction of mutual coupling between closely-spaced microstrip antennas. In *20th Iranian Conference on Electrical Engineering (ICEE)*. Tehran (Iran), 2012, p. 1347–1350. DOI: 10.1109/IranianCEE.2012.6292566

[13] PEDRAM, K., NOURINIA, J., GHOBADI, C. A small dual band antenna with simple structure for WLAN/WIMAX application. In *8th International Symposium on Telecommunications (IST)*. Tehran (Iran), 2016, p. 349–352. DOI: 10.1109/ISTEL.2016.7881838

[14] PALANDOKEN, M. Compact bioimplantable MICS and ISM band antenna design for wireless biotelemetry applications. *Radioengineering*, 2017, vol. 26, no. 4, p. 917–923. DOI: 10.13164/re.2017.091

[15] PAN, B. C., CUI, T. J. Broadband decoupling network for dual-band microstrip patch antennas. *IEEE Transactions on Antennas and Propagation*, 2017, vol. 65, no. 10, p. 5595–5598. DOI: 10.1109/TAP.2017.2742539

[16] MONTI, A., SORIC, J., BARBUTO, M., et al. Mantle cloaking for co-site radio-frequency antennas. *Applied Physics Letters*, 2016, vol. 108, no. 11, p. 1–5, article ID 113502. DOI: 10.1063/1.4944042

[17] JIANG, Z., SIEBER, P. E., KANG, L., et al. Restoring intrinsic properties of electromagnetic radiators using ultralightweight integrated metasurface cloaks. *Advanced Functional Materials*, 2015, vol. 25, no. 29, p. 4708–4716. DOI: 10.1002/adfm.201501261

[18] VELLUCI, S., MONTI, A., BARBUTO, M., et al. Satellite applications of electromagnetic cloaking. *IEEE Transactions on Antennas and Propagation*, 2017, vol. 65, no. 9, p. 4931–4934. DOI: 10.1109/TAP.2017.2722865

[19] IBRAHIM, A. A., ABDALLA, M. A. CRLH MIMO antenna with reversal configuration. *AEU-International Journal of Electronics and Communications*, 2016, vol. 70, no. 9, p. 1134–1141. DOI: 10.1016/j.aeue.2016.05.012

About the Authors …

Negin POUYANFAR was born in Iran. She received her B.Sc. and M.Sc. degrees in Electrical Engineering from the Islamic Azad University. She is currently a Ph.D. candidate of Telecommunication Engineering in Urmia University, Urmia, Iran. Her research interests include multiband and MIMO antenna design, metasurfaces and metamaterial antennas.

Changiz GHOBADI was born in June, 1960 in Iran. He received his B.Sc. in Electrical Engineering Electronics and M.Sc. degrees in Electrical Engineering Telecommunication from Isfahan University of Technology, Isfahan, Iran and Ph.D. degree in Electrical-Telecommunication from the University of Bath, Bath, UK in 1998. From 1998 he was an Assistant Professor and now he is a Professor in the Department of Electrical Engineering of Urmia University, Urmia, Iran. His primary research interests are in antenna design, radar and adaptive filters.

Javad NOURINIA received his B.Sc. in Electrical and Electronic Engineering from Shiraz University and M.Sc. degree in Electrical and Telecommunication Engineering from the Iran University of Science and Technology, and Ph.D. degree in Electrical and Telecommunication from the University of Science and Technology, Tehran, Iran in 2000. From 2000 he was an Assistant Professor and now he is a Professor in the Department of Electrical Engineering of Urmia University, Urmia, Iran. His primary research interests are in antenna design, numerical methods in electromagnetic, microwave circuits.

Kioumars PEDRAM was born in Iran. He received his B.Sc. in Electrical Engineering from Bonab University and M.Sc. Degree in Telecommunication Engineering from Urmia University. His research interests include antenna design, microwave circuits, metamaterials, metasurfaces, SIW structures and MIMO antennas.

Maryam MAJIDZADEH was born in 1987 in Urmia, Iran. She received her B.Sc. in Electrical Engineering from Urmia University in 2009. As well, she received her M.Sc. and Ph.D. degrees in Communication Engineering from the same university in 2012 and 2016, respectively. She is now an assistant professor in the Department of Electrical and Computer Engineering, Urmia Girls Faculty, West Azarbaijan branch, Technical and Vocational University (TVU), Urmia, Iran. Her research interests include antenna design, antenna miniaturization techniques, MIMO antenna design, frequency selective surfaces and electromagnetic compatibility.